

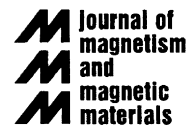


ELSEVIER

Available online at www.sciencedirect.com

ScienceDirect

Journal of Magnetism and Magnetic Materials 320 (2008) e175–e178

www.elsevier.com/locate/jmmm

Phase transitions in Heusler alloys with exchange inversion

V.D. Buchelnikov^{a,*}, S.V. Taskaev^a, M.A. Zagrebin^a, V.V. Khovailo^b, P. Entel^c

^aChelyabinsk State University, Chelyabinsk 454021, Russian Federation

^bInstitute of Radioengineering and Electornics of RAS, Moscow 125009, Russian Federation

^cPhysics Department, University of Duisburg-Essen, Lotharstr. 1, Duisburg Campus, 47048 Duisburg, Germany

Available online 21 February 2008

Abstract

Phase diagrams of the Heusler Ni–Mn–X (X = In, Sn, Sb) alloys with exchange inversion are investigated. It is shown that a few different types of the phase diagrams depending on the signs of phenomenological parameters of the Ginzburg–Landau functional are obtained. In the diagrams there are thermodynamic paths, which can explain the experimentally observed sequences of the phase transitions in Ni–Mn–X alloys.

© 2008 Elsevier B.V. All rights reserved.

PACS: 64.60.–i; 64.70.Kb; 75.50.Cc

Keywords: Heusler alloys; Structural and magnetic phase transitions; Exchange inversion

It is known that in some Heusler alloys a magnetoelastic interaction lead to a change of sign of the exchange interaction. In this case the phase transition occurs from ferromagnetic state to antiferromagnetic one. In the Heusler alloys this transition is accompanied with the martensitic one. For instance this phenomena observed in Ni–Mn–X (X = In, Sn, Sb) Heusler alloys [1,2]. These materials have much better mechanical properties. Stresses of over 100 MPa are generated in the external field of 70 kOe. Such stress levels are approximately 50 times larger than that generated in the previous shape-memory alloys [3]. These materials are interesting for engineering of different devices and hence their potential for applications is significantly enhanced.

According to the Ginzburg–Landau theory we can write the free energy of a cubic antiferromagnet in the following form [4]:

$$F = \tilde{A}L^2/2 + \tilde{B}L^4/4 + A_1M^2/2 + \tilde{D}(ML)^2/2 \\ + D'M^2L^2/2 + K(L_x^2L_y^2 + L_y^2L_z^2 + L_x^2L_z^2) \\ + K'(M_x^2M_y^2 + M_y^2M_z^2 + M_x^2M_z^2) - \mathbf{MH}$$

$$+ B_0e_1L^2 + G_0e_1M^2 + B_1[e_2(L_x^2 - L_y^2)/2 \\ + e_3(3L_z^2 - L^2)/\sqrt{6}] \\ + G_1[e_2(M_x^2 - M_y^2)/2 + e_3(3M_z^2 - M^2)/\sqrt{6}] \\ + B_2[e_4L_xL_y + e_5L_yL_z + e_6L_xL_z] \\ + G_2[e_4M_xM_y + e_5M_yM_z + e_6M_xM_z] \\ - Ee_1 + E_0e_1^2/2 + a_1(e_2^2 + e_3^2)/2 \\ + C_{44}(e_4^2 + e_5^2 + e_6^2)/2 + E_1e_1(e_2^2 + e_3^2) \\ + b_1e_3(e_3^2 - 3e_2^2)/3 + c_1(e_2^2 + e_3^2)^2/4. \quad (1)$$

Here e_i are the linear combinations of the deformation tensor components, $e_1 = (e_{xx} + e_{yy} + e_{zz})/\sqrt{3}$, $e_2 = (e_{xx} - e_{yy})/\sqrt{2}$, $e_3 = (2e_{zz} - e_{yy} - e_{xx})/\sqrt{6}$, $e_4 = e_{xy}$, $e_5 = e_{yz}$, $e_6 = e_{zx}$; $M = (M_1 + M_2)/2M_0$, $L = (M_1 - M_2)/2M_0$ are the moduli of vectors of ferro- and antiferromagnetism, where M_1 , M_2 are the moduli of sublattice magnetization vectors and M_0 is the saturation magnetization; E is a coefficient proportional to the thermal expansion coefficient, $E_0 = (c_{11} + 2c_{12})/\sqrt{3}$ is the bulk modulus, a_1 , b_1 , E_1 , c_1 are the linear combinations of the second-, third-, and fourth-order elastic moduli, respectively, $a_1 = c_{11} - c_{12}$, $b_1 = (c_{111} - c_{112} + 2c_{123})/6\sqrt{6}$, $E_1 = (c_{111} - c_{123})/2\sqrt{3}$, $c_1 = (c_{1111} + 6c_{1112} - 3c_{1122} - 8c_{1233})/48$; B_i and G_i are the magnetoelastic constants; K and K' are the magnetic anisotropy

*Corresponding author. Tel.: +7 351 799 7117; fax: +7 351 742 0925.

E-mail address: buche@csu.ru (V.D. Buchelnikov).

constants; \tilde{A} , \tilde{B} , A_1 , \tilde{D} , D' are the exchange interaction parameters. Considering the case of antiferromagnetism we should introduce the angle φ between the magnetization vectors \mathbf{M}_1 and \mathbf{M}_2 . Neglecting the magnetic anisotropy and anisotropic magnetoelastic interaction we renormalize the coefficients of the expression (1) with the account of the equilibrium values of the deformations e_1 , e_4 , e_5 , e_6 . As a result we can obtain the following expression for the density of the free energy:

$$F = A \cos \varphi + B \cos^2 \varphi + D \cos \varphi (e_2^2 + e_3^2)/2 + a(e_2^2 + e_3^2)/2 + be_3(e_3^2 - 3e_2^2)/3 + c(e_2^2 + e_3^2)^2/4. \quad (2)$$

For optimizing numerical calculations of the phase diagrams we pass to the dimensionless variables for (2)

$$\bar{F} = c^3 F/b^4, \quad \bar{e}_{2,3} = ce_{2,3}/|b|, \quad \bar{A} = c^3 A/b^4, \quad \bar{B} = c^3 B/b^4, \quad \bar{D} = cD/b^2, \quad \bar{a} = ca/b^2. \quad (3)$$

For the simplification we will use the redefined constants without bars over them. The final expression for the density of the free energy will reduce to the form

$$F = A \cos \varphi + B \cos^2 \varphi + D \cos \varphi (e_2^2 + e_3^2)/2 + a(e_2^2 + e_3^2)/2 + \text{sign } be_3(e_3^2 - 3e_2^2)/3 + (e_2^2 + e_3^2)^2/4. \quad (4)$$

To find all possible equilibrium states of Eq. (4), it is necessary to minimize Ginzburg–Landau functional taking into account all order parameters e_2 , e_3 , and φ , which are responsible for the structural and magnetic phase transitions. The minimization of the functional (4) leads to nine equilibrium states.

1. The FM cubic phase (FC) $\varphi = 0$, $e_2 = e_3 = 0$. It is stable when $A \leq -2B$, $a \geq -D$.
2. The FM tetragonal phase (FT) $\varphi = 0$, $e_2 = 0$, $e_3 = e_T = (-\text{sign } b \pm (1-4(a+D))^{1/2})/2$.
3. The FM orthorhombic phase (FR) $\varphi = 0$, $e_2^2 = 3e_3^2$, $e_3 = e_R = (\text{sign } b \pm (1-4(a+D))^{1/2})/4$.
- The FM tetragonal and orthorhombic phases have the same region of stability which is bordered by the following inequalities $A \leq -2B - (D/8)(1 + (1-4(a+D))^{1/2})^2$ and $a \leq 1/4 - D$.
4. The AFM cubic phase (AFC) $\varphi = \pi$, $e_2 = e_3 = 0$. It is stable when $A \geq 2B$, $a \geq D$.
5. The AFM tetragonal phase (AFT) $\varphi = \pi$, $e_2 = 0$, $e_3 = e_{AT} = (-\text{sign } b \pm (1-4(a-D))^{1/2})/2$.
6. The AFM orthorhombic phase (AFR) $\varphi = \pi$, $e_2^2 = 3e_3^2$, $e_3 = e_{AR} = (\text{sign } b \pm (1-4(a-D))^{1/2})/4$.

The AFM tetragonal and orthorhombic phases have the same region of stability which is bordered by the following inequalities $A \geq 2B - (D/8)(1 + (1-4(a-D))^{1/2})^2$ and $a \leq 1/4 + D$.

7. The AFM angular cubic phase (CAFC) $\cos \varphi = -A/2B$, $e_2 = e_3 = 0$. It is stable when $A \geq -2B$, $A \leq 2B$, $B \geq 0$, $a \geq DA/2B$.

8. The AFM angular tetragonal phase (CAFT) $\cos \varphi = -(A + De_3^2/2)/2B$, $e_2 = 0$, $e_3 = e_{CT} = (-\text{sign } b \pm (1-4a'c')^{1/2})/2c'$.
9. The AFM angular orthorhombic phase (CAFR) $\cos \varphi = -(A + D(e_2^2 + e_3^2)/2)/2B$, $e_2^2 = 3e_3^2$, $e_3 = e_{CR} = (\text{sign } b \pm (1-4a'c')^{1/2})/4c'$.

The AFM angular tetragonal and orthorhombic phases have the same region of stability which is bordered by the following inequalities $A \geq -2B - (D/8)(1 + (1-4(a+D))^{1/2})^2$, $a \leq 1/4 - D$, $A \leq 2B - (D/8)(1 + (1-4(a-D))^{1/2})^2$, $a \leq 1/4 + D$, $A \geq 2Ba/D - B/(2c'D)$ and $B \geq D^2/4$. Here $a' = a - DA/2B$ and $c' = 1 - D^2/4B$.

The sign of the parameter b determines only the sign of e_3 deformations and does not change the type of the phase diagram. With $b > 0$ e_3 deformations are positive in FR, AFR, CAFR phases and they are negative in FT, AFT, and CAFT ones. With $b < 0$ the signs of e_3 deformations in these phases are inverse. The stability regions of the phases also prove that angular antiferromagnetic phases exist only with positive values of the parameter B . When the parameter B is negative in alloys with the inversion of exchange interaction six possible states can exist: three ferromagnetic (FC, FT, FR) and three antiferromagnetic (AFC, AFT, AFR) phases. The angular CAFT and CAFR phases occur when $B \geq D^2/4$.

Lines of phase transitions can be determined from equality of energy of phases. They have form

- 1–2(3) $a = 2/9 - D$;
- 1–4 $A = 0$;
- 1–5(6) $A = (1/24)|e_{AT}|^3(2-3|e_{AT}|)$;
- 1–7 $A = -2B$;
- 1–8(9) $A = -2B \pm ((1/3)B|e_{CT}|^3(2-3c'|e_{CT}|))^{1/2}$, $A \leq 2Ba/D - 4B/(9Dc')$;
- 2–4 $A = (1/24)|e_T|^3(3|e_T|-2)$;
- 2–5(6) $A = (1/24)(|e_{AT}|^3(2-3|e_{AT}|) - |e_T|^3(2-3|e_T|))$;
- 2–7 $A = -2B \pm ((1/3)B|e_T|^3(3|e_T|-2))^{1/2}$, $a < 2/9 - D$;
- 2–8(9) $A = \pm ((1/3)B[|e_{CT}|^3(2-3c'|e_{CT}|) - |e_T|^3(2-3|e_T|)])^{1/2} - 2B$, $|e_{CT}|^3(2-3c'|e_{CT}|) - |e_T|^3(2-3|e_T|) \geq 0$;
- 4–5(6) $a = 2/9 + D$;
- 4–7 $A = 2B$;
- 4–8(9) $A = 2B \pm ((1/3)B|e_{CT}|^3(2-3c'|e_{CT}|))^{1/2}$, $A \leq 2Ba/D - 4B/(9Dc')$, $a \leq 2/9 + D$;
- 5–8(9) $A = \pm ((1/3)B[|e_{CT}|^3(2-3c'|e_{CT}|) - |e_{AT}|^3(2-3|e_{AT}|)])^{1/2} + 2B$, $|e_{CT}|^3(2-3c'|e_{CT}|) - |e_{AT}|^3(2-3|e_{AT}|) \geq 0$;
- 7–8(9) $A = 2Ba/D - 4B/(9Dc')$.

The phase (A – a) diagram for the case when $B < 0$, $D > 0$ is schematically presented in Fig. 1. Here and below solid lines correspond to the lines of phase transitions and dashed lines determined the regions of phase stability. From Fig. 1 follow that in this case six possible states can exist: FC, FT, FR, AFC, AFT and AFR. The FC phase is stable in the region bordered with LG and GW lines. The AFC phase is stable in the region placed to the right of PM

Download English Version:

<https://daneshyari.com/en/article/1803075>

Download Persian Version:

<https://daneshyari.com/article/1803075>

[Daneshyari.com](https://daneshyari.com)